Please cite this article in press as: Kwon *et al*., Isoliquiritigenin Induces Apoptosis via ROS-Mediated Inhibition of p38/mTOR/STAT3 Pathway in Human Melanoma Cells, Biomol. Ther. (2025), https://doi.org/10.4062/biomolther.2024.118

BIOMOLECULES & THERAPEUTICS

Original Article
Biomol Ther, 1-10 (2025)

Isoliquiritigenin Induces Apoptosis via ROS-Mediated Inhibition of p38/mTOR/STAT3 Pathway in Human Melanoma Cells

Mi Jeong Kwon[1,†], Pawan Kumar Raut[1,†], Jeong-Hoon Jang[2,*] and Kyung-Soo Chun[1,*]

[1]*College of Pharmacy, Keimyung University, Daegu 42601,*
[2]*College of Pharmacy, Daegu Catholic University, Gyeongsan 38430, Republic of Korea*

Abstract

Isoliquiritigenin (ISL), a phenolic compound derived from licorice, exhibits various biological activities, including anti-inflammatory, anti-viral, anti-tumor, and antioxidant effects. However, the molecular mechanisms underlying its anti-cancer effects are not well understood in SK-MEL-28 melanoma cells. Melanoma, a highly aggressive and treatment-resistant cancer, remains a significant health challenge. This study investigates the anti-cancer effects of ISL, focusing on identifying reactive oxygen species (ROS)-mediated apoptosis mechanisms on SK-MEL-28 melanoma cells. Our results show that ISL treatment induces apoptosis in SK-MEL-28 cells, as evidenced by the cleavage of caspase-9, -7, -3, and PARP. ISL increased Bax expression, decreased Bcl-2 expression, and promoted cytochrome C release into the cytosol. ISL also reduced the expression of cell cycle markers, including cyclin D1, D3, and survivin. Notably, ISL treatment markedly increased intracellular ROS levels and pretreatment with *N*-acetyl cysteine, a ROS scavenger, abrogated the ISL-induced inhibition of the p38/mTOR/STAT3 pathway and prevented apoptosis. Moreover, ISL significantly diminished the constitutive phosphorylation of mTOR and STAT3 in SK-MEL-28 cells by blocking the phosphorylation of p38 MAPK, an upstream kinase of mTOR. Pharmacological inhibition of mTOR attenuated the STAT3 signaling, indicating that mTOR acts as an upstream kinase of STAT3 in these cells. Collectively, these findings demonstrate that ISL inhibits SK-MEL-28 cell growth by downregulating cell survival proteins and inducing apoptosis through ROS generation.

Key Words: Isoliquiritigenin, SK-MEL-28 cells, ROS, Melanoma, Apoptosis

INTRODUCTION

Melanoma, a malignancy of melanocytes, accounts for a small percentage of skin cancer but contributes to a higher mortality rate. It is estimated that 99,780 new cases of melanoma were diagnosed, and 7,650 individuals died from melanoma in the US (Siegel *et al*., 2022). Although the incidence of melanoma has stabilized since 2019 (Siegel *et al*., 2023), it remains a significant health challenge. The survival rate for stage IV melanoma has also improved in recent years due to systemic therapies utilizing BRAF/MEK inhibitors and immunotherapy (Miller *et al*., 2022). Despite these advances, melanoma still has a poor prognosis, posing ongoing challenges for treatment (Franklin *et al*., 2017). Therefore, developing new chemotherapeutic agents with low toxicity and potent anti-tumor activity is crucial for managing melanoma (Ye *et al*., 2016; Obrador *et al*., 2019).

Reactive oxygen species (ROS) are unstable, oxygen-containing reactive species predominantly generated in mitochondria and other organelles such as peroxisomes and the endoplasmic reticulum (Perillo *et al*., 2020). NADPH oxidases, membrane-bound proteins, also play a critical role in converting oxygen to superoxide free radicals (Bedard and Krause, 2007). ROS act as second messengers within cells and are essential for maintaining cellular homeostasis. Studies have shown that low to moderate levels of ROS production are necessary for cancer cell survival, while higher levels induce cancer cell death (Yang *et al*., 2018). Many anti-cancer agents inhibit cancer cell growth by inducing oxidative stress (Chun and Joo, 2022; Jiang *et al*., 2023). Oxidative stress can trigger various types of cell death, including apoptosis, ferroptosis, autophagy, and necroptosis, through different signaling mech-

Open Access **https://doi.org/10.4062/biomolther.2024.118**

Received Jul 21, 2024 **Revised** Sep 23, 2024 **Accepted** Oct 8, 2024
Published Online Feb 12, 2025

***Corresponding Authors**
E-mail: chunks@kmu.ac.kr (Chun KS), jhjang17@cu.ac.kr (Jang JH)
Tel: +82-53-580-6647 (Chun KS), +82-53-850-3612 (Jang JH)
Fax: +82-53-715-2028 (Chun KS), +82-53-359-6613 (Jang JH)
[†]The first two authors contributed equally to this work.

anisms. For instance, ROS contribute to apoptosis by causing mitochondrial damage and activating ASK1 and PARP (Villalpando-Rodriguez and Gibson, 2021).

The mammalian target of rapamycin (mTOR) is a serine/threonine kinase that regulates critical cellular processes such as protein synthesis, metabolism, aging, and regeneration. Activation of mTOR signaling can induce cell survival, cytoskeletal rearrangement, invasion, metastasis, apoptosis inhibition, and autophagy inhibition (Murugan, 2019). Several upstream kinases, including phosphoinositide 3-kinase (PI3K)/AKT, mitogen-activated protein kinase (MAPK), and vascular endothelial growth factor (VEGF), can activate mTOR signaling in response to different stimuli (Conciatori *et al*., 2018). p38 MAPK are tyrosine-protein kinases that play crucial roles in transcription, protein synthesis, cell-surface receptor expression, regulation of cell cycle proteins, and apoptosis (Bulavin and Fornace, 2004). Inactivation of the p38 MAPK pathway can inhibit cell growth and induce apoptosis by negatively regulating cell survival pathways (Coulthard *et al*., 2009).

Isoliquiritigenin (ISL), a bioactive compound derived from licorice species (*Glycyrrhiza uralensis*, *Glycyrrhiza glabra*, and *Glycyrrhiza inflata*), possesses various pharmacological properties, including anti-inflammatory, anti-ulcer, anti-bacterial, and anti-tumor effects (Wang *et al*., 2020). Previous studies have demonstrated that ISL exhibits potent anti-cancer activities against cervical, breast, liver, colon, and prostate cancers (Peng *et al*., 2015). ISL exerts its anti-tumor properties by inhibiting carcinogenic processes such as growth, proliferation, angiogenesis, invasion, and migration (Peng *et al*., 2015; Zhang *et al*., 2022). The tumor-suppressive effects of ISL are mediated through cell cycle arrest and apoptotic induction via various signaling pathways, including PI3K/AKT, JAK/STAT3, ERK, and NF-κB (Hsu *et al*., 2005; Zhang *et al*., 2010; Li *et al*., 2013; Wang *et al*., 2019). However, the effect of ISL on SK-MEL-28 melanoma cells and the ROS-mediated underlying molecular mechanisms remain elusive.

This study aimed to investigate the anti-cancer effects of ISL in SK-MEL-28 melanoma cells, focusing on identifying novel ROS-related molecular mechanisms. We found that ISL attenuated the growth of SK-MEL-28 cells *in vitro* by elevating ROS levels. The increased ROS levels induced by ISL led to reduced expression of cyclins and the induction of apoptosis through the inhibition of the p38/mTOR/STAT3 signaling pathway.

MATERIALS AND METHODS

Chemicals and reagents

All cell culture reagents were procured from Hyclone Laboratories (Logan, UT, USA). ISL, *N*-acetyl cysteine (NAC), and primary antibody against β-actin were purchased from Sigma-Aldrich (St. Louis, MO, USA). Primary antibodies specific for cleaved caspase-9, caspase-7, caspase-3, cleaved poly (ADP-ribose) polymerase (PARP), mTOR, p-mTOR (Ser2448), STAT3, p-STAT3 (Ser727), cytochrome C, cyclin D1 and D3, NOX1 and 2, and secondary antibodies conjugated with horseradish peroxidase (HRP) were obtained from Cell Signaling Technology Inc. (Beverly, MA, USA). Primary antibodies against, Bcl-2, Bax, p38, and p-p38 (Thr180/Tyr182) were procured from Santa Cruz Biotechnology (Dallas, TX, USA). Primary survivin antibody was obtained from Novus Biologicals (Littleton, CO, USA). Primary antibody specific for COX IV were purchased from Abcam (Cambridge, MA, USA). The 2'-7'-dichlorofluorescein diacetate (DCF-DA) and mitochondria/cytosol fractionation kit were purchased from Invitrogen (Carlsbad, CA, USA).

Cell culture

SK-MEL-28, a human non-pigmented melanoma cell line, was obtained from the American Type Culture Collection (Manassas, VA, USA) and routinely cultured in Dulbecco's Modified Eagle Medium supplemented with 10% fetal bovine serum and antibiotics (100 U/mL penicillin G and 100 mg/mL streptomycin) at 37°C in a humidified incubator containing 5% CO_2 and 95% air.

Measurement of cell viability (MTT assay)

The effect of ISL on cell growth was measured using a 3-(4,5-dimethylthiazol-2-yl)-2,5-diphenyltetrazolium bromide (MTT) assay (Shakya *et al*., 2023). Briefly, cells (2×10^3) were seeded in triplicate in a 96-well plate and cultured overnight. The cells were then treated with ISL at the concentrations indicated in the figure legends. Next, 10 μL of MTT solution (5 mg/mL) was added to each well and incubated for 4 h. The media was removed, and the insoluble formazan was dissolved in DMSO. The absorbance was measured at 550 nm using a microplate reader (Tecan Trading AG, Männedorf, Switzerland). Cell viability/growth is expressed as the relative percentage of the control.

Annexin V staining

Annexin V staining was performed using the FITC-Annexin V staining kit (BD Biosciences, San Jose, CA, USA) following the manufacturer's instructions. Briefly, cells were treated with ISL in the presence or absence of NAC as indicated in the figure legends. The cells were harvested, washed with PBS, and resuspended in binding buffer containing Annexin V and propidium iodide (PI). Fluorescence intensity was determined using fluorescence-activated cell sorting (FACS) (BD Biosciences).

Western blot analysis

Total cellular extracts were prepared by lysing the cells in RIPA buffer containing halt protease inhibitor. Total protein concentrations of cell lysates were quantified using a bicinchoninic acid protein assay kit (Pierce Biotechnology, Rockford, IL, USA). For immunoblot analysis, 30-50 μg of total protein was separated using 10-15% (w/v) SDS-PAGE gel and transferred to a polyvinylidene difluoride membrane. The membranes were blocked using 5% (w/v) skim milk in Tris-buffered saline with Tween-20 for 1 h at room temperature (RT). The membranes were then incubated with primary antibodies (1:1,000 dilutions in 3% BSA) overnight at 4°C, followed by incubation with secondary antibodies conjugated with HRP (1:5,000) for 1 h at RT. Chemiluminescent images of protein-antibody complexes were visualized using SuperSignal WesternBright ECL HRP substrate (Advansta, San Jose, CA, USA) or SuperSignal™ West Femto maximum sensitivity substrate (Thermo Fisher Scientific, Waltham, MA USA) according to the manufacturer's instructions and visualized with an ImageQuant™ LAS 4000 (Fujifilm Life Science, Tokyo, Japan).

Measurement of ROS production

Total intracellular ROS production was measured by assessing changes in the fluorescence of DCF-DA as described previously (Shakya *et al*., 2023). Briefly, cells were treated with ISL in the presence or absence of NAC and then incubated with 25 μM of DCF-DA for 30 min in the dark at 37°C. Cells were washed twice with PBS to remove excess DCF-DA, and intracellular ROS levels were examined under a fluorescence microscope. Total ROS production was quantified using the ImageJ program (National Institutes of Health, Bethesda, MD, USA).

Isolation of mitochondrial and cytoplasmic protein

To examine changes in the protein expression of apoptotic proteins, cytoplasmic and mitochondrial protein fractions were prepared after treating SK-MEL-28 cells with ISL using the Mitochondria/Cytosol Fractionation Kit (BioVision Inc., Milpitas, CA, USA) as described previously (Sim *et al*., 2024). Briefly, 1.5×10^6 cells were seeded overnight and treated with ISL as indicated in the figure legends. The cells were washed with ice-cold PBS and centrifuged at 600 g for 5 min at 4°C. The cells were resuspended in cytosolic buffer and incubated on ice for 10 min. The homogenate was prepared by passing the cell suspension through a Dounce homogenizer. The homogenate was centrifuged at 700 g for 10 min at 4°C, and the supernatant was further centrifuged at 10,000 g for 30 min at 4°C. The supernatant was considered the cytosolic fraction. The pellet was resuspended in mitochondrial extraction buffer mix and vortexed for 10 sec to prepare the mitochondrial fraction. The levels of cytochrome C in the cytoplasm and mitochondria were determined by Western blot analysis as described.

Luciferase reporter gene assay

A dual-luciferase reporter assay system (Promega, Madison, WI, USA) was used for the luciferase reporter assay for STAT3, as described previously (Raut and Park, 2020; Sim *et al*., 2024). Briefly, SK-MEL-28 cells were seeded at a density of 3×10^5 cells/well onto a six-well plate. After overnight incubation, cells were cotransfected with STAT3 and renilla luciferase plasmids using FuGENE HD transfection reagent (Promega) for 24 h, following the manufacturer's instructions. The cells were further stimulated with the indicated ISL concentrations for 24 h. The cells were lysed with passive lysis buffer and centrifuged at 13,000 rpm for 10 min to obtain a whole-cell lysate. Finally, the luminescence of firefly and renilla was identified by adding luciferase assay reagent and Stop & Glo reagent, respectively, in 20 μL of cell lysate using a multimode microplate reader (Tecan, Mannedorf, Switzerland). The values are expressed relative to the controls after normalization with renilla luciferase because the renilla luciferase plasmid acts as an internal loading control for transfection efficiency.

Statistical analysis

All experiments were conducted in at least triplicate, and data are presented as the mean ± standard deviation (SD) from independent experiments. Statistical analysis was performed using the ANOVA test to compare the differences between groups. A *p*-value less than 0.05 was considered statistically significant.

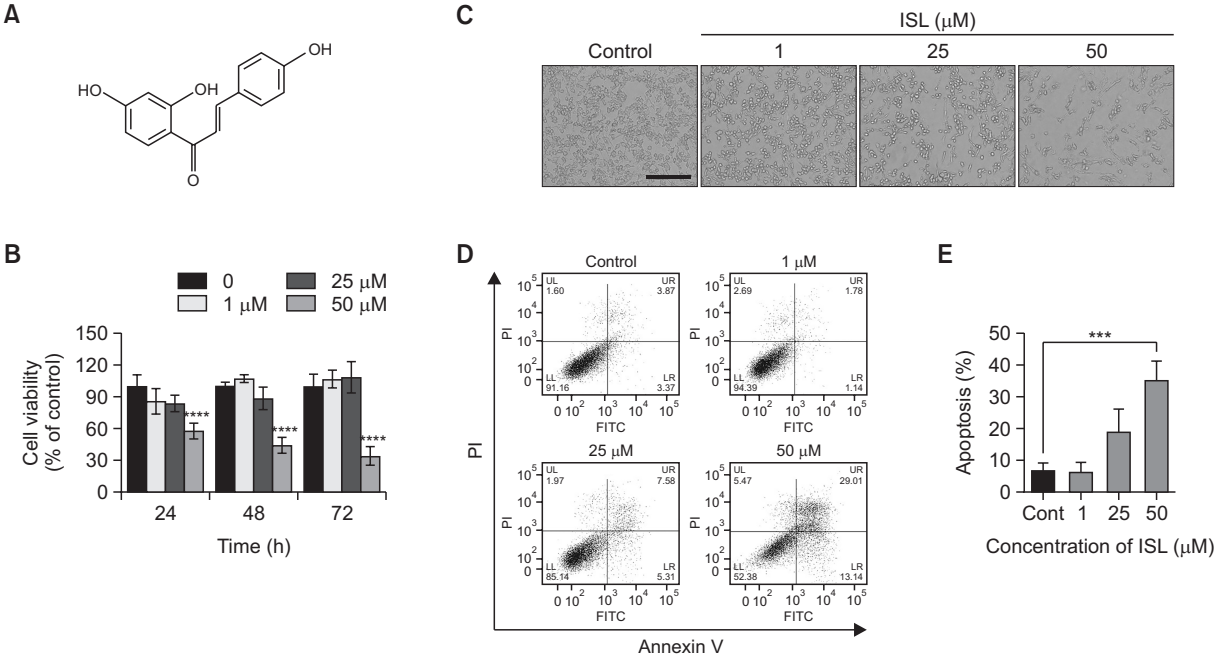

Fig. 1. Effects of ISL on SK-MEL-28 cell viability and apoptotic induction. (A) Chemical structure of ISL. (B) SK-MEL-28 cells were treated with ISL (1, 25, and 50 μM) for 24, 48, and 72 h, and cell viability was determined using the MTT cell viability assay. Data are shown as the mean ± SD (n=3). (C) Representative images of ISL-treated SK-MEL-28 cells. The scale bar indicates 200 μm. (D, E) Apoptosis in SK-MEL-28 cells, treated with varying ISL concentrations (1, 25, and 50 μM) for 48 h, was analyzed using FACS with Annexin V/PI staining. Data are shown as the mean ± SD (n=3). ***p<0.001, ****p<0.0001.

RESULTS

ISL induces apoptosis in SK-MEL-28 cells

Several studies have demonstrated that ISL exhibits anti-cancer activities both *in vitro* and *in vivo* (Wu *et al*., 2016; Song *et al*., 2020; Yu *et al*., 2023). The chemical structure of ISL is shown in Fig. 1A. We first assessed the effect of ISL on the viability of SK-MEL-28 cells by MTT assay. Treatment with ISL (1, 25, and 50 μM) resulted in reduction of cell viability, with higher concentrations of ISL decreasing viability in a time-dependent manner, as shown in Fig. 1B. Specifically, treatment with 50 μM of ISL reduced cell growth by 60% compared to the vehicle-treated control. Additionally, Fig. 1C shows significant morphological changes in SK-MEL-28 cells following incubation with varying concentrations of ISL. To investigate the occurrence of apoptosis in ISL-treated cells, we performed FACS to quantify the population of apoptotic cells by double staining with Annexin V and PI. The results indicated that ISL treatment significantly increased the percentage of apoptotic cells compared to vehicle-treated control, as shown in Fig. 1D and 1E. Collectively, these findings suggest that ISL suppresses the growth of SK-MEL-28 melanoma cells through the induction of apoptosis.

ISL mediates apoptosis via activation of the mitochondrial pathway in SK-MEL-28 cells

To investigate the mechanisms underlying ISL-induced apoptosis in SK-MEL-28 cells, we examined the activation of key apoptotic markers. As shown in Fig. 2A, treatment with ISL (1, 25, and 50 μM) resulted in the activation of caspase-9, -7, and -3, as well as the cleavage of PARP, indicating the involvement of the mitochondrial pathway in ISL-induced apoptosis. Given the role of Bcl-2 family proteins in regulating mitochondrial membrane integrity, we next assessed the effect of ISL on the expression of these proteins. ISL treatment reduced the expression of Bcl-2 while significantly increasing the expression of Bax, an apoptotic protein, in SK-MEL-28 cells (Fig. 2B). This imbalance between Bcl-2 and Bax led to elevated levels of cytochrome C in the whole cell lysate following ISL treatment, as shown in Fig. 2B. Several studies have reported that the translocation of cytochrome C from the mitochondria to the cytoplasm is a hallmark of apoptosis (Wang, 2001). We investigated the effect of ISL on this translocation and found that ISL treatment significantly increased the level of cytochrome C in the cytoplasm while concurrently decreasing its level in the mitochondria, as shown in Fig. 2C. This result confirms the translocation of cytochrome C from the mitochondria to the cytoplasm upon ISL exposure in SK-MEL-28 cells. Furthermore, ISL treatment reduced the expression of survivin and D-series cyclins, including cyclin D1 and cyclin D3, indicating that ISL inhibits cell cycle progression in SK-MEL-28 cells (Fig. 2D). Collectively, these results reveal that ISL attenuates the growth of SK-MEL-28 cells by inducing apoptosis and arresting the cell cycle.

ISL treatment induces apoptosis via ROS production in SK-MEL-28 cells

Increasing evidence highlights the pivotal role of ROS in the mechanism of action of anti-cancer agents. To further explore this, we investigated the effect of ISL on ROS generation

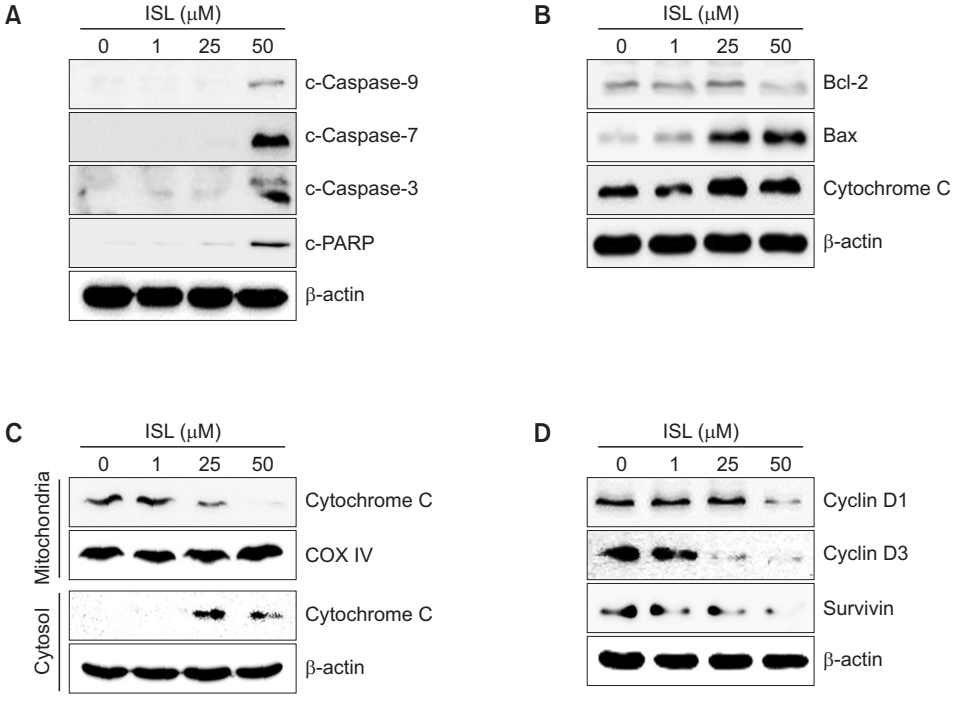

Fig. 2. Activation of apoptotic pathways and inhibition of cell cycle-related proteins by ISL in SK-MEL-28 cells. (A) Immunoblot analysis of cleaved forms of caspase-3, -7, and -9 and PARP protein levels. (B) Immunoblot analysis of mitochondrial apoptosis-related proteins Bcl-2, Bax, and cytochrome C in SK-MEL-28 cells. (C) Immunoblot analysis of mitochondrial apoptosis-related protein cytochrome C in the mitochondrial and cytosolic fractions of SK-MEL-28 cells and COX IV was used as the loading control for mitochondrial proteins. (D) Immunoblot analysis of cell cycle-related proteins cyclin D1, D3, and survivin. β-Actin was used as the loading control.

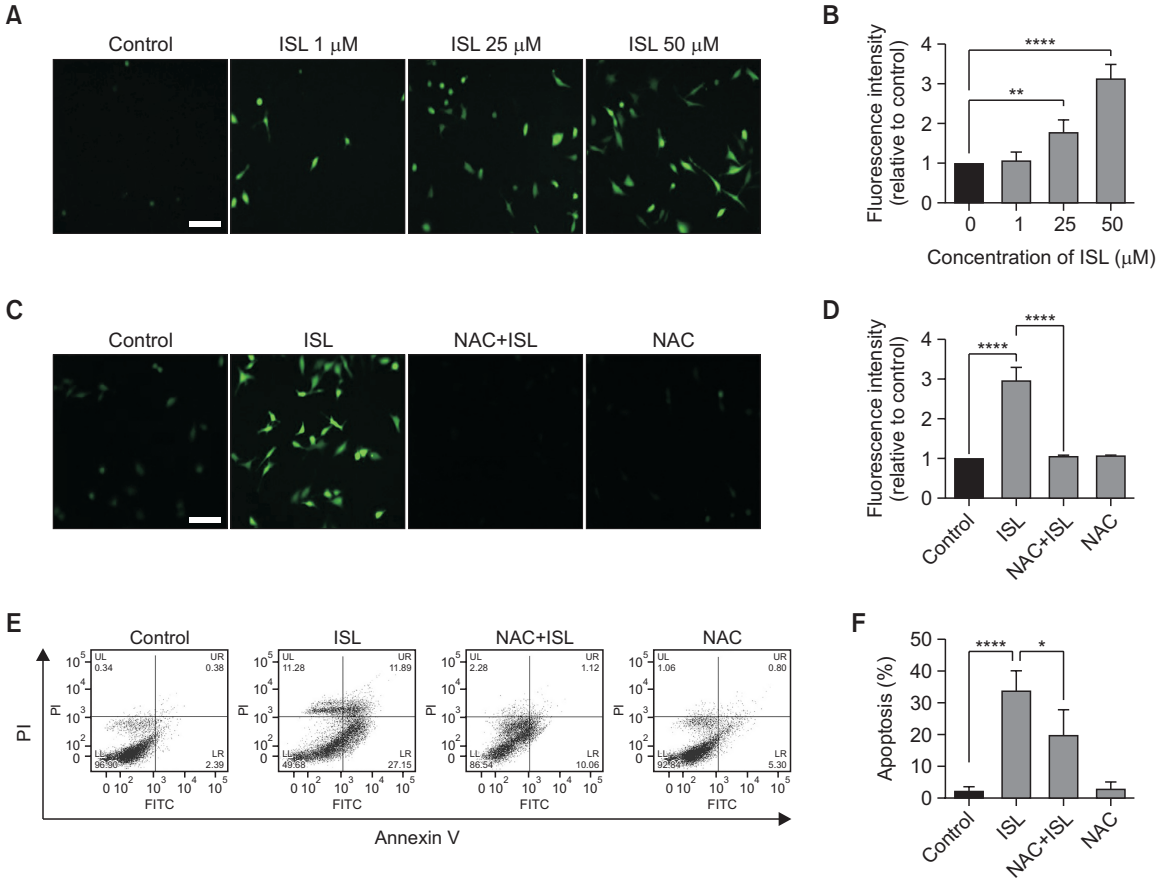

Fig. 3. ISL-induced ROS production as a mediator of apoptosis in SK-MEL-28 cells. (A-D) The intracellular accumulation of ROS was identified by measuring the fluorescence of DCF-DA using fluorescence microscopy in SK-MEL-28 cells after ISL treatment. (A, C) Representative DCF-DA fluorescence microscopic images. The scale bar indicates 200 μm. (B, D) Graph of DCF-DA fluorescence intensity. (E, F) SK-MEL-28 cells were pretreated with the ROS scavenger NAC (5 mM) for 1 h before exposure to ISL (50 μM) for 4 h. Apoptosis in SK-MEL-28 cells, treated with ISL and/or NAC, was analyzed using FACS with Annexin V/PI staining. Data are shown as the mean ± SD (n=3). **p*<0.05, ***p*<0.01, *****p*<0.0001.

in SK-MEL-28 cells. As shown in Fig. 3A and 3B, ISL treatment (1, 25, 50 μM) for 4 h significantly elevated intracellular ROS production in a dose-dependent manner, suggesting its involvement in regulating cell death and downstream signaling events. Additionally, pretreatment with NAC, a ROS scavenger, markedly reduced ISL-induced ROS accumulation and the associated apoptosis in SK-MEL-28 cells (Fig. 3C-3F). These observations indicate that ISL-induced ROS production is a key mediator of apoptosis in SK-MEL-28 cells. Collectively, these findings demonstrate that ISL exposure leads to a dramatic increase in ROS production, which in turn facilitates the induction of apoptosis in SK-MEL-28 cells.

ROS production regulates the genes related to apoptosis and cyclins expression by ISL in SK-MEL-28 cells

The ISL-induced ROS generation resulted in apoptosis induction, as indicated in Fig. 3E. To further explore the role of ROS in regulating apoptosis-related genes and cyclins in SK-MEL-28 cells, we examined the effects of ROS production. As shown in Fig. 4A, pretreatment with NAC significantly diminished the ISL-induced cleavage of caspase-9, -7, -3, and PARP. Moreover, the ISL-induced downregulation of Bcl-2 expression and upregulation of Bax expression were reversed by NAC pretreatment, as illustrated in Fig. 4B. Similarly, pretreatment with NAC substantially reduced the ISL-induced increase in cytochrome C levels in SK-MEL-28 cells (Fig. 4B). These results collectively indicate that ROS plays a crucial role in apoptosis induction by modulating the expression of Bax, an apoptotic protein, and Bcl-2, an anti-apoptotic protein, in SK-MEL-28 cells upon ISL exposure. Furthermore, the ISL-induced suppression of survivin and cyclins, including cyclin D1 and cyclin D3, was almost restored to normal levels with NAC pretreatment in SK-MEL-28 cells (Fig. 4C). This finding underscores the importance of ROS in the downregulation of survivin and cyclins, highlighting its critical role in the regulation of cell cycle and apoptosis in response to ISL treatment.

ISL inactivates p38-mTOR-STAT3 signaling pathway in SK-MEL-28 cells via ROS production

The regulation of key signaling proteins such as p38, mTOR, and STAT3 plays a crucial roles in cancer cell survival and proliferation (Song *et al*., 2015; Martínez-Limón *et al*., 2020; Panwar *et al*., 2023; Phan *et al*., 2023). ROS have been implicated in modulating these kinases, influencing both

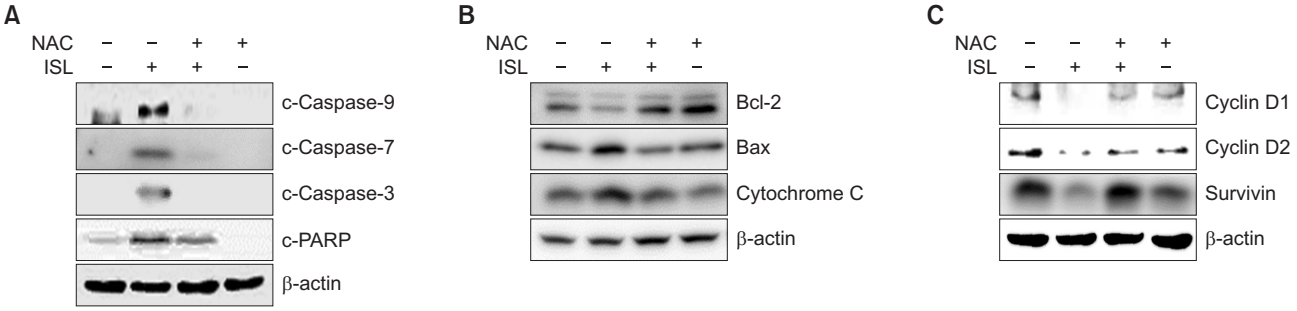

Fig. 4. Role of ROS in ISL-mediated apoptotic pathways and cell cycle-related proteins in SK-MEL-28 cells. SK-MEL-28 cells were pretreated with the ROS scavenger NAC (5 mM) for 1 h before exposure to ISL (50 μM) for 48 h. (A) Immunoblot analysis of cleaved forms of caspase-3, -7, and -9 and PARP protein levels. (B) Immunoblot analysis of mitochondrial apoptosis-related proteins Bcl-2, Bax, and cytochrome C in SK-MEL-28 cells. (C) Immunoblot analysis of cell cycle-related proteins cyclin D1, D3, and survivin. β-Actin was used as the loading control.

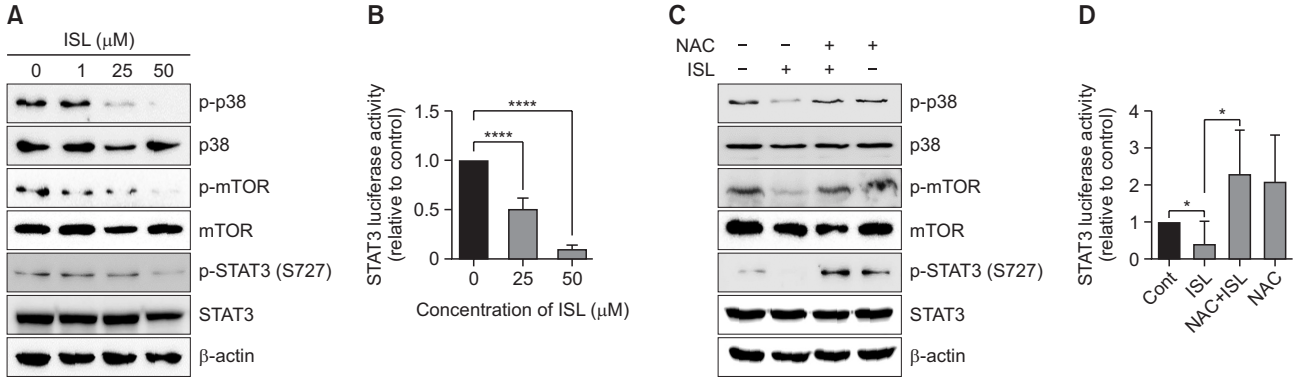

Fig. 5. Inactivation of p38/mTOR/STAT3 signaling by ISL via ROS production in SK-MEL-28 cells. (A, B) SK-MEL-28 cells were treated with ISL (1, 25, and 50 μM) for 48 h. (A) Immunoblot analysis of p38, mTOR, and STAT3 proteins. (B) STAT3 reporter gene activity in response to ISL. Values are presented as the mean ± SD (n=3). (C, D) SK-MEL-28 cells were pretreated with the ROS scavenger NAC (5 mM) for 1 h before exposure to ISL (50 μM) for 48 h. (C) Immunoblot analysis of p38, mTOR, and STAT3 proteins. (D) SK-MEL-28 cells were pretreated with the ROS scavenger NAC (5 mM) for 1 h before exposure to ISL (50 μM) for 48 h. Values are presented as the mean ± SD (n=3). **p*<0.05, *****p*<0.0001.

canonical and non-canonical apoptosis signaling mechanisms within the cancer cells (Redza-Dutordoir and Averill-Bates, 2016; Lee *et al*., 2021). It has been established that p38 MAPK can act upstream of the mammalian target of rapamycin (mTOR) kinase (Hernández *et al*., 2011), and mTOR can regulate the signal transducer and activator of transcription 3 (STAT3) under various experimental conditions (Zhou *et al*., 2007). We investigated the effect of ISL on the activation of several kinases, including p38 and mTOR. As shown in Fig. 5A, ISL treatment significantly reduced the constitutive phosphorylation of both p38 and mTOR in a concentration-dependent manner in SK-MEL-28 cells, indicating that ISL inactivates these pathways. Similarly, ISL treatment decreased the phosphorylation of STAT3 at serine 727, a non-canonical activation site, without affecting the overall STAT3 levels (Fig. 5A). Moreover, ISL markedly reduced STAT3 luciferase reporter activity in a concentration-dependent manner (Fig. 5B). Given that ROS production can regulate various kinases (Zhang *et al*., 2016), we examined the impact of ROS on p38, mTOR, and STAT3 phosphorylation under ISL treatment. Interestingly, the ISL-induced decrease in phosphorylated p38 and mTOR was dramatically reversed by pretreatment with NAC in SK-MEL-28 cells (Fig. 5C). Similarly, NAC pretreatment restored the ISL-induced reduction in p-STAT3 levels (Fig. 5C). Since ISL increases intracellular ROS production and inhibits non-canonical STAT3 signaling, we further investigated the effect of ROS on STAT3 activity using a gene reporter assay. As shown in Fig. 5D, NAC pretreatment significantly restored the ISL-induced decrease in STAT3 gene reporter activity. Collectively, these results indicate that ISL inhibits several kinases, including p38, mTOR, and STAT3, through a ROS-dependent mechanism.

p38/mTOR/STAT3 signaling regulates cyclins expression in SK-MEL-28 cells

Given that p38 MAPK can act upstream of mTOR and STAT3 (Xu *et al*., 2018), we investigated the effect of SB203580, a selective inhibitor of p38 MAPK, on activation of downstream kinases, including mTOR and STAT3. As shown in Fig. 6A, treating SK-MEL-28 cells with SB203580 for 24 h drastically decreased the phosphorylation of p38, mTOR, and STAT3 (Ser727) in a concentration-dependent manner. This finding suggests that p38 MAPK acts as an upstream regulator of both mTOR and STAT3 in these cells. Additionally, the

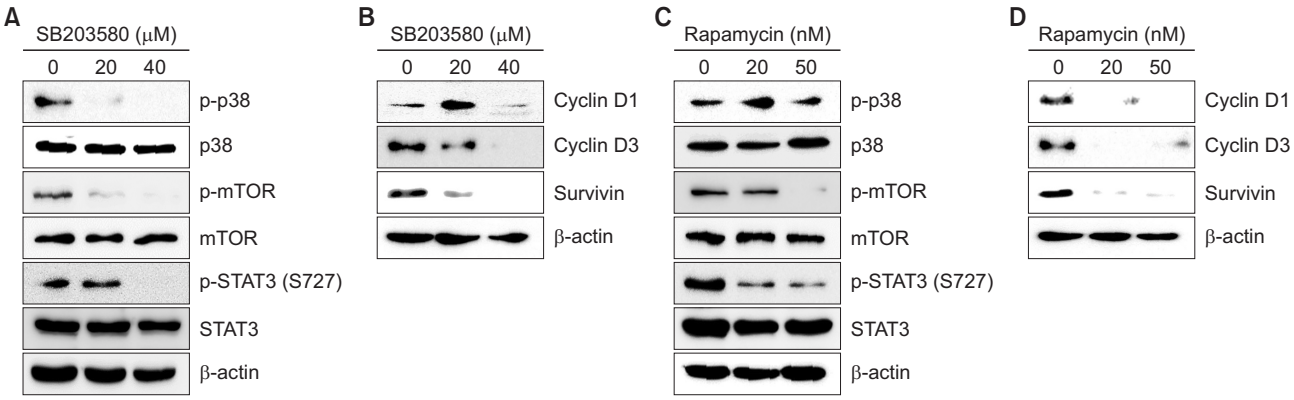

Fig. 6. Modulation of cyclins expression and survivin by p38/mTOR/STAT3 pathway inhibition in SK-MEL-28 cells. (A-D) SK-MEL-28 cells were treated with either SB203580 or rapamycin for 24 h. (A) Immunoblot analysis of p38, mTOR, and STAT3 proteins. (B) Immunoblot analysis of cell cycle-related proteins cyclin D1, D3, and survivin. (C) Immunoblot analysis of p38, mTOR, and STAT3 proteins. (D) Immunoblot analysis of cell cycle-related proteins cyclin D1, D3, and survivin. β-Actin served as the loading control.

expression levels of cyclin D1, cyclin D3, and survivin were significantly reduced following SB203580 treatment (Fig. 6B). To further elucidate the pathway, we treated SK-MEL-28 cells with rapamycin, a mTOR inhibitor, at concentrations of 20 and 50 nM for 24 h. As shown in Fig. 6C, rapamycin treatment abrogated the phosphorylation of mTOR and STAT3 (Ser727), but did not affect p38 phosphorylation. This clearly indicates that mTOR regulates the non-canonical STAT3 pathway but does not influence the p38 MAPK pathway in SK-MEL-28 cells. Furthermore, rapamycin treatment also dramatically reduced the expression of survivin and cyclins, including cyclin D1 and cyclin D3, similar to the effects observed with SB203580 (Fig. 6D). These findings collectively indicate that the p38/mTOR/STAT3 signaling pathway plays a critical role in regulating the expression of survivin and cyclins in SK-MEL-28 cells (Fig. 7). Understanding the precise modulation of this pathway provides valuable insights and may offer promising therapeutic targets for controlling the proliferation and survival of melanoma cells.

DISCUSSION

Cancer poses a significant health challenge globally, with around 19.5 million new cases and 0.6 million deaths annually in the USA alone (Siegel *et al*., 2023). Although various chemotherapeutic and biological agents have been developed, their clinical application is often limited by systemic toxicities (Basak *et al*., 2021). Phytochemicals, naturally occurring compounds in plants, have gained attention due to their potent anti-cancer activities with minimal systemic toxicity (Choudhari *et al*., 2019; Choi *et al*., 2023; Hwang *et al*., 2023; Kim *et al*., 2023). ISL, a natural flavonoid from licorice, is known for its anti-inflammatory and antioxidant properties (Yu *et al*., 2018). This study explores the anti-cancer effects of ISL on SK-MEL-28 human melanoma cells, revealing its growth inhibitory effects and underlying molecular mechanisms.

ISL treatment has shown a concentration-dependent induction of apoptosis in SK-MEL-28 cells, consistent with other cancer cell studies (Wu *et al*., 2016; Chen *et al*., 2017). Specifically, ISL induces the cleavage of executioner caspases, including caspase-9, -3, and -7, leading to the cleavage of PARP. This indicates the activation of the intrinsic apoptosis pathway, marked by the translocation of cytochrome C from mitochondria to the cytoplasm. Additionally, ISL increased ROS levels, which further promoted apoptosis and suppressed the expression of cyclins by inhibiting the p38/mTOR/STAT3 signaling pathway in SK-MEL-28 cells. This finding aligns with previous reports where ISL follows the intrinsic pathway of apoptosis in various cancer cell types (Jung *et al*., 2006; Hirchaud *et al*., 2013; Chen *et al*., 2017; Kim *et al*., 2017; Tian *et al*., 2018; Luo *et al*., 2023).

ROS play a dual role in cancer, with moderate levels promoting growth and high levels inducing cell death (Newsholme *et al*., 2016; Perillo *et al*., 2020). ISL significantly increases ROS production in SK-MEL-28 cells, leading to apoptosis and cell growth suppression. This is evident from the elevated intracellular ROS levels following ISL treatment. A moderate increase in ROS levels usually favors the growth and progression of cancer. However, excess production of ROS is known to affect the structure and function of cellular proteins and lipids, leading to cellular dysfunction, including impaired energy metabolism, altered cell signaling, and cell cycle disruption, subsequently resulting in cell death. The ISL-induced ROS production appears to be a critical factor in its anti-cancer mechanism, as pretreatment with NAC, a ROS scavenger, reduces ISL-induced apoptosis and cyclin expression suppression (Kim *et al*., 2017). These findings suggest that ROS play a crucial role in ISL's anti-cancer effects, although its impact may vary across different cancer cell types and experimental conditions. Notably, our data demonstrate that treatment of SK-MEL-28 cells with ISL significantly upregulated the expression of NOX1, a NADPH oxidase isoform involved in ROS production, indicating that the ISL-induced ROS production might be NOX1-dependent in this experimental condition (Supplementary Fig. 1). However, further studies exploring the role of ROS induced by ISL in various cancer subtypes are essential for a better understanding.

In our study, ISL treatment also resulted in the suppression of the p38 MAPK/mTOR/STAT3 signaling pathways in SK-MEL-28 cells. p38 MAPK is involved in various cellular processes, including apoptosis and cell migration, and its in-

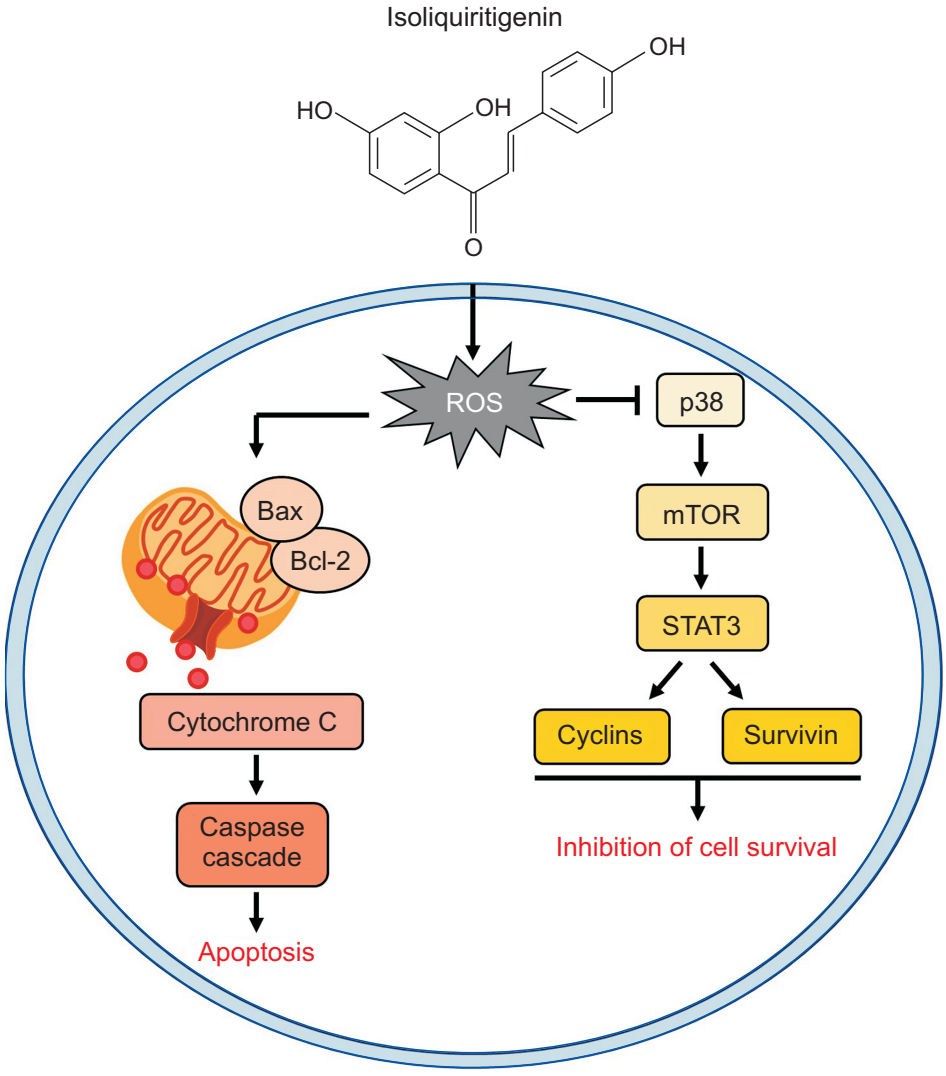

Fig. 7. Schematic Representation of ISL-induced apoptosis mechanisms in SK-MEL-28 cells via p38/mTOR/STAT3 signaling and ROS generation.

hibition leads to the suppression of cancer cell growth (Martínez-Limón *et al*., 2020). ISL inhibits the phosphorylation of p38 MAPK and mTOR, which in turn downregulates STAT3 activation, a key transcription factor in cell proliferation and survival. This suppression is consistent with ISL's effects in other cancer cell types, where it inhibits the PI3K/AKT/mTOR pathways (Zhang *et al*., 2022). Similarly, LPS-induced p38 MAPK was remarkably decreased with the treatment of ISL in MAC-T bovine mammary epithelial cells (Li *et al*., 2022). To the best of our knowledge, this is the first report demonstrating that the p38 MAPK/mTOR pathway plays a critical role in ISL-induced cell death of melanoma cells. STAT3, a transcription factor, is well known to regulate genes associated with cell proliferation and survival, including cyclins, Myc, Bcl-2, and Bcl-xl, to promote the growth of cancer cells (Huynh *et al*., 2019). ISL treatment has been shown to arrest the growth of Caki renal cancer cells via ROS-mediated inactivation of the JAK2/STAT3 signaling pathway (Kim *et al*., 2017). Similarly, our study demonstrated that ISL resulted in the abrogation of p38 MAPK/mTOR/STAT3 signaling in SK-MEL-28 cells. Treatment of SK-MEL-28 cells with rapamycin, an inhibitor of mTOR, significantly reduced the phosphorylated forms of mTOR and STAT3 (Ser727), as well as cyclin D1, cyclin D3, and survivin, indicating that ISL inhibits cyclins and survivin in a non-canonical STAT3-dependent manner. Furthermore, the study demonstrated that ISL-induced ROS production mediates the inactivation of p38 MAPK/mTOR/STAT3 signaling pathways. This ROS-dependent mechanism highlights the central role of oxidative stress in ISL's anti-cancer activity. Pretreatment with NAC reversed the ISL-induced inhibition of these pathways, underscoring the importance of ROS in mediating these effects. Additionally, ISL treatment reduced the expression of cyclin D1, D3, and survivin, further indicating its role in cell cycle arrest and apoptosis induction in SK-MEL-28 cells.

Typically, ROS generation is known to promote the activation of MAPK pathways, including p38 (Son *et al*., 2011). However, the effect of ROS on MAPK activation is dynamic

and context dependent. A study reports that increased ROS production can inhibit p38 MAPK activation in the context of melanocyte apoptosis (Tang *et al*., 2019). Additionally, another research has shown that ROS can activate the phosphatase DUSP1, a negative regulator of MAPKs, including p38, thereby reducing their activation (Liu *et al*., 2008). These findings suggest that the relationship between ROS and p38 MAPK may vary depending on cellular context and conditions. Further studies are required to elucidate the precise mechanisms governing ROS and p38 MAPK interactions across different cellular environments and disease states.

In conclusion, this study provides substantial evidence that ISL inhibits the growth of SK-MEL-28 melanoma cells by inducing apoptosis through a ROS-dependent mechanism. The inactivation of the p38 MAPK/mTOR/STAT3 signaling pathways further elucidates the molecular basis of ISL's anti-cancer effects. These findings suggest that ISL could be a promising therapeutic agent for treating human melanoma, offering a potential approach with minimal systemic toxicity compared to conventional chemotherapeutic agents. By highlighting the molecular pathways affected by ISL, this study enhances our understanding of its anti-cancer mechanisms and supports further research into its potential therapeutic applications in melanoma and other cancers.

CONFLICT OF INTEREST

The authors report no declarations of interest. The authors alone are responsible for the content and writing of the paper.

ACKNOWLEDGMENTS

This research was funded by the Bisa Research Grant of Keimyung University in 2023 (Project No: 20230327).

REFERENCES

Basak, D., Arrighi, S., Darwiche, Y. and Deb, S. (2021) Comparison of anticancer drug toxicities: paradigm shift in adverse effect profile. *Life (Basel)* **12**, 48.

Bedard, K. and Krause, K. H. (2007) The NOX family of ROS-generating NADPH oxidases: physiology and pathophysiology. *Physiol. Rev.* **87**, 245-313.

Bulavin, D. V. and Fornace, A. J., Jr. (2004) p38 MAP kinase's emerging role as a tumor suppressor. *Adv. Cancer Res.* **92**, 95-118.

Chen, H. Y., Huang, T. C., Shieh, T. M., Wu, C. H., Lin, L. C. and Hsia, S. M. (2017) Isoliquiritigenin induces autophagy and inhibits ovarian cancer cell growth. *Int. J. Mol. Sci.* **18**, 2025-2039.

Choi, Y., Park, S., Lee, S., Shin, H. E., Kwon, S., Choi, J. K., Lee, M. H., Seo, S. Y. and Lee, Y. (2023) Cremastranone-derived homoisoflavanes suppress the growth of breast cancer cells via cell cycle arrest and caspase-independent cell death. *Biomol. Ther. (Seoul)* **31**, 526-535.

Choudhari, A. S., Mandave, P. C., Deshpande, M., Ranjekar, P. and Prakash, O. (2019) Phytochemicals in cancer treatment: from preclinical studies to clinical practice. *Front. Pharmacol.* **10**, 1614.

Chun, K. S. and Joo, S. H. (2022) Modulation of reactive oxygen species to overcome 5-fluorouracil resistance. *Biomol. Ther. (Seoul)* **30**, 479-489.

Conciatori, F., Ciuffreda, L., Bazzichetto, C., Falcone, I., Pilotto, S., Bria, E., Cognetti, F. and Milella, M. (2018) mTOR cross-talk in cancer and potential for combination therapy. *Cancers* **10**, 23-52.

Coulthard, L. R., White, D. E., Jones, D. L., McDermott, M. F. and Burchill, S. A. (2009) p38(MAPK): stress responses from molecular mechanisms to therapeutics. *Trends Mol. Med.* **15**, 369-379.

Franklin, C., Livingstone, E., Roesch, A., Schilling, B. and Schadendorf, D. (2017) Immunotherapy in melanoma: recent advances and future directions. *Eur. J. Surg. Oncol.* **43**, 604-611.

Hernández, G., Lal, H., Fidalgo, M., Guerrero, A., Zalvide, J., Force, T. and Pombo, C. M. (2011) A novel cardioprotective p38-MAPK/mTOR pathway. *Exp. Cell Res.* **317**, 2938-2949.

Hirchaud, F., Hermetet, F., Ablise, M., Fauconnet, S., Vuitton, D. A., Prétet, J. L. and Mougin, C. (2013) Isoliquiritigenin induces caspase-dependent apoptosis via downregulation of HPV16 E6 expression in cervical cancer Ca Ski cells. *Planta Med.* **79**, 1628-1635.

Hsu, Y. L., Kuo, P. L. and Lin, C. C. (2005) Isoliquiritigenin induces apoptosis and cell cycle arrest through p53-dependent pathway in Hep G2 cells. *Life Sci.* **77**, 279-292.

Huynh, J., Chand, A., Gough, D. and Ernst, M. (2019) Therapeutically exploiting STAT3 activity in cancer - using tissue repair as a road map. *Nat. Rev. Cancer* **19**, 82-96.

Hwang, S. Y., Wi, K., Yoon, G., Lee, C. J., Lee, S. I., Jung, J. G., Jeong, H. W., Kim, J. S., Choi, C. H., Na, C. S., Shim, J. H. and Lee, M. H. (2023) Licochalcone D inhibits skin epidermal cells transformation through the regulation of AKT signaling pathways. *Biomol. Ther. (Seoul)* **31**, 682-691.

Jiang, H., Zuo, J., Li, B., Chen, R., Luo, K., Xiang, X., Lu, S., Huang, C., Liu, L., Tang, J. and Gao, F. (2023) Drug-induced oxidative stress in cancer treatments: angel or devil? *Redox Biol.* **63**, 102754.

Jung, J. I., Lim, S. S., Choi, H. J., Cho, H. J., Shin, H. K., Kim, E. J., Chung, W. Y., Park, K. K. and Park, J. H. (2006) Isoliquiritigenin induces apoptosis by depolarizing mitochondrial membranes in prostate cancer cells. *J. Nutr. Biochem.* **17**, 689-696.

Kim, D. H., Park, J. E., Chae, I. G., Park, G., Lee, S. and Chun, K. S. (2017) Isoliquiritigenin inhibits the proliferation of human renal carcinoma Caki cells through the ROS-mediated regulation of the Jak2/STAT3 pathway. *Oncol. Rep.* **38**, 575-583.

Kim, N., Kwon, J., Shin, U. S. and Jung, J. (2023) Stimulatory anticancer effect of resveratrol mediated by G protein-coupled estrogen receptor in colorectal cancer. *Biomol. Ther. (Seoul)* **31**, 655-660.

Lee, S. O., Joo, S. H., Kwak, A. W., Lee, M. H., Seo, J. H., Cho, S. S., Yoon, G., Chae, J. I. and Shim, J. H. (2021) Podophyllotoxin induces ROS-mediated apoptosis and cell cycle arrest in human colorectal cancer cells via p38 MAPK signaling. *Biomol. Ther. (Seoul)* **29**, 658-666.

Li, M., Lu, G., Ma, X., Wang, R., Chen, X., Yu, Y. and Jiang, C. (2022) Anti-inflammation of isoliquiritigenin via the inhibition of NF-κB and MAPK in LPS-stimulated MAC-T cells. *BMC Vet. Res.* **18**, 320.

Li, Y., Zhao, H., Wang, Y., Zheng, H., Yu, W., Chai, H., Zhang, J., Falck, J. R., Guo, A. M., Yue, J., Peng, R. and Yang, J. (2013) Isoliquiritigenin induces growth inhibition and apoptosis through downregulating arachidonic acid metabolic network and the deactivation of PI3K/Akt in human breast cancer. *Toxicol. Appl. Pharmacol.* **272**, 37-48.

Liu, Y. X., Wang, J., Guo, J., Wu, J., Lieberman, H. B. and Yin, Y. (2008) DUSP1 is controlled by p53 during the cellular response to oxidative stress. *Mol. Cancer Res.* **6**, 624-633.

Luo, F., Tang, Y., Zheng, L., Yang, Y., Gao, H., Tian, S., Chen, H., Tang, C., Tang, S., Man, Q. and Wu, Y. (2023) Isoliquiritigenin inhibits the growth of colorectal cancer cells through the ESR2/PI3K/AKT signalling pathway. *Pharmaceuticals (Basel)* **17**, 43.

Martínez-Limón, A., Joaquin, M., Caballero, M., Posas, F. and de Nadal, E. (2020) The p38 pathway: from biology to cancer therapy. *Int. J. Mol. Sci.* **21**, 1913.

Miller, K. D., Nogueira, L., Devasia, T., Mariotto, A. B., Yabroff, K. R., Jemal, A., Kramer, J. and Siegel, R. L. (2022) Cancer treatment and survivorship statistics, 2022. *CA Cancer J. Clin.* **72**, 409-436.

Murugan, A. K. (2019) mTOR: role in cancer, metastasis and drug resistance. *Semin. Cancer Biol.* **59**, 92-111.

Newsholme, P., Cruzat, V. F., Keane, K. N., Carlessi, R. and de Bittencourt, P. I., Jr. (2016) Molecular mechanisms of ROS production and oxidative stress in diabetes. *Biochem. J.* **473**, 4527-4550.

Obrador, E., Liu-Smith, F., Dellinger, R. W., Salvador, R., Meyskens,

F. L. and Estrela, J. M. (2019) Oxidative stress and antioxidants in the pathophysiology of malignant melanoma. *Biol. Chem.* **400**, 589-612.

Panwar, V., Singh, A., Bhatt, M., Tonk, R. K., Azizov, S., Raza, A. S., Sengupta, S., Kumar, D. and Garg, M. (2023) Multifaceted role of mTOR (mammalian target of rapamycin) signaling pathway in human health and disease. *Signal Transduct. Target. Ther.* **8**, 375.

Peng, F., Du, Q., Peng, C., Wang, N., Tang, H., Xie, X., Shen, J. and Chen, J. (2015) A review: the pharmacology of isoliquiritigenin. *Phytother. Res.* **29**, 969-977.

Perillo, B., Di Donato, M., Pezone, A., Di Zazzo, E., Giovannelli, P., Galasso, G., Castoria, G. and Migliaccio, A. (2020) ROS in cancer therapy: the bright side of the moon. *Exp. Mol. Med.* **52**, 192-203.

Phan, T., Zhang, X. H., Rosen, S. and Melstrom, L. G. (2023) P38 kinase in gastrointestinal cancers. *Cancer Gene Ther.* **30**, 1181-1189.

Raut, P. K. and Park, P. H. (2020) Globular adiponectin antagonizes leptin-induced growth of cancer cells by modulating inflammasomes activation: critical role of HO-1 signaling. *Biochem. Pharmacol.* **180**, 114186.

Redza-Dutordoir, M. and Averill-Bates, D. A. (2016) Activation of apoptosis signalling pathways by reactive oxygen species. *Biochim. Biophys. Acta* **1863**, 2977-2992.

Shakya, R., Byun, M. R., Joo, S. H., Chun, K. S. and Choi, J. S. (2023) Domperidone exerts antitumor activity in triple-negative breast cancer cells by modulating reactive oxygen species and JAK/STAT3 signaling. *Biomol. Ther. (Seoul)* **31**, 692-699.

Siegel, R. L., Miller, K. D., Fuchs, H. E. and Jemal, A. (2022) Cancer statistics, 2022. *CA Cancer J. Clin.* **72**, 7-33.

Siegel, R. L., Miller, K. D., Wagle, N. S. and Jemal, A. (2023) Cancer statistics, 2023. *CA Cancer J. Clin.* **73**, 17-48.

Sim, S. J., Jang, J. H., Choi, J. S. and Chun, K. S. (2024) Domperidone, a dopamine receptor D2 antagonist, induces apoptosis by inhibiting the ERK/STAT3-mediated pathway in human colon cancer HCT116 cells. *Biomol. Ther. (Seoul)* **32**, 568-576.

Son, Y., Cheong, Y. K., Kim, N. H., Chung, H. T., Kang, D. G. and Pae, H. O. (2011) Mitogen-activated protein kinases and reactive oxygen species: how can ROS activate MAPK pathways? *J. Signal. Transduct.* **2011**, 792639.

Song, H. M., Park, G. H., Eo, H. J., Lee, J. W., Kim, M. K., Lee, J. R., Lee, M. H., Koo, J. S. and Jeong, J. B. (2015) Anti-proliferative effect of naringenin through p38-dependent downregulation of cyclin D1 in human colorectal cancer cells. *Biomol. Ther. (Seoul)* **23**, 339-344.

Song, L., Luo, Y., Li, S., Hong, M., Wang, Q., Chi, X. and Yang, C. (2020) ISL induces apoptosis and autophagy in hepatocellular carcinoma via downregulation of PI3K/AKT/mTOR pathway *in vivo* and *in vitro*. *Drug Des. Devel. Ther.* **14**, 4363-4376.

Tang, L., Li, J., Fu, W., Wu, W. and Xu, J. (2019) Suppression of FADS1 induces ROS generation, cell cycle arrest, and apoptosis in melanocytes: implications for vitiligo. *Aging (Albany N.Y.)* **11**, 11829-11843.

Tian, T., Sun, J., Wang, J., Liu, Y. and Liu, H. (2018) Isoliquiritigenin inhibits cell proliferation and migration through the PI3K/AKT signaling pathway in A549 lung cancer cells. *Oncol. Lett.* **16**, 6133-6139.

Villalpando-Rodriguez, G. E. and Gibson, S. B. (2021) Reactive oxygen species (ROS) regulates different types of cell death by acting as a rheostat. *Oxid. Med. Cell. Longev.* **2021**, 9912436.

Wang, T. T., Chen, Z. Z., Xie, P., Zhang, W. J., Du, M. Y., Liu, Y. T., Zhu, H. Y. and Guo, Y. S. (2019) Isoliquiritigenin suppresses the proliferation and induced apoptosis via miR-32/LATS2/Wnt in nasopharyngeal carcinoma. *Eur. J. Pharmacol.* **856**, 172352.

Wang, X. (2001) The expanding role of mitochondria in apoptosis. *Genes Dev.* **15**, 2922-2933.

Wang, Z. F., Liu, J., Yang, Y. A. and Zhu, H. L. (2020) A review: the anti-inflammatory, anticancer and antibacterial properties of four kinds of Licorice flavonoids isolated from Licorice. *Curr. Med. Chem.* **27**, 1997-2011.

Wu, C. H., Chen, H. Y., Wang, C. W., Shieh, T. M., Huang, T. C., Lin, L. C., Wang, K. L. and Hsia, S. M. (2016) Isoliquiritigenin induces apoptosis and autophagy and inhibits endometrial cancer growth in mice. *Oncotarget* **7**, 73432-73447.

Xu, X., Zhi, T., Chao, H., Jiang, K., Liu, Y., Bao, Z., Fan, L., Wang, D., Li, Z., Liu, N. and Ji, J. (2018) ERK1/2/mTOR/Stat3 pathway-mediated autophagy alleviates traumatic brain injury-induced acute lung injury. *Biochim. Biophys. Acta Mol. Basis Dis.* **1864**, 1663-1674.

Yang, H., Villani, R. M., Wang, H., Simpson, M. J., Roberts, M. S., Tang, M. and Liang, X. (2018) The role of cellular reactive oxygen species in cancer chemotherapy. *J. Exp. Clin. Cancer Res.* **37**, 266.

Ye, T., Zhu, S., Zhu, Y., Feng, Q., He, B., Xiong, Y., Zhao, L., Zhang, Y., Yu, L. and Yang, L. (2016) Cryptotanshinone induces melanoma cancer cells apoptosis via ROS-mitochondrial apoptotic pathway and impairs cell migration and invasion. *Biomed. Pharmacother.* **82**, 319-326.

Yu, D., Liu, X., Zhang, G., Ming, Z. and Wang, T. (2018) Isoliquiritigenin inhibits cigarette smoke-induced COPD by attenuating inflammation and oxidative stress via the regulation of the Nrf2 and NF-kappaB signaling pathways. *Front. Pharmacol.* **9**, 1001.

Yu, M., Pan, Q., Li, W., Du, T., Huang, F., Wu, H., He, Y., Wu, X. and Shi, H. (2023) Isoliquiritigenin inhibits gastric cancer growth through suppressing GLUT4 mediated glucose uptake and inducing PDHK1/PGC-1α mediated energy metabolic collapse. *Phytomedicine* **121**, 155045.

Zhang, J., Wang, X., Vikash, V., Ye, Q., Wu, D., Liu, Y. and Dong, W. (2016) ROS and ROS-mediated cellular signaling. *Oxid. Med. Cell. Longev.* **2016**, 4350965.

Zhang, X., Yeung, E. D., Wang, J., Panzhinskiy, E. E., Tong, C., Li, W. and Li, J. (2010) Isoliquiritigenin, a natural anti-oxidant, selectively inhibits the proliferation of prostate cancer cells. *Clin. Exp. Pharmacol. Physiol.* **37**, 841-847.

Zhang, Z., Chen, W. Q., Zhang, S. Q., Bai, J. X., Liu, B., Yung, K. K. and Ko, J. K. (2022) Isoliquiritigenin inhibits pancreatic cancer progression through blockade of p38 MAPK-regulated autophagy. *Phytomedicine* **106**, 154406.

Zhou, J., Wulfkuhle, J., Zhang, H., Gu, P., Yang, Y., Deng, J., Margolick, J. B., Liotta, L. A., Petricoin, E., 3rd and Zhang, Y. (2007) Activation of the PTEN/mTOR/STAT3 pathway in breast cancer stem-like cells is required for viability and maintenance. *Proc. Natl. Acad. Sci. U. S. A.* **104**, 16158-16163.